

This all-or-none phenomenon may seem surprising when one considers that  $\text{Na}^+$  conductance increases in a strictly *graded* manner as depolarization increases (Figure 10–6). Each increment of depolarization increases the number of voltage-gated  $\text{Na}^+$  channels that open, thereby gradually increasing  $\text{Na}^+$  current. How then can there be a discrete threshold for generating an action potential?

Although a small subthreshold depolarization increases the inward  $I_{\text{Na}}$ , it also increases two *outward* currents,  $I_{\text{K}}$  and  $I_{\text{L}}$ , by increasing the electrochemical driving forces acting on  $\text{K}^+$  and  $\text{Cl}^-$ . In addition, the depolarization augments  $\text{K}^+$  conductance by gradually opening more voltage-gated  $\text{K}^+$  channels (Figure 10–6). As the outward  $\text{K}^+$  and leakage currents increase with depolarization, they tend to repolarize the membrane and thereby resist the depolarizing action of the  $\text{Na}^+$  influx. However, because of the high voltage sensitivity and more rapid kinetics of activation of the  $\text{Na}^+$  channels, the depolarization eventually reaches the point at which the increase in inward  $I_{\text{Na}}$  exceeds the increase in outward  $I_{\text{K}}$  and  $I_{\text{L}}$ . At this point, there is a net inward ionic current. This produces a further depolarization, opening even more  $\text{Na}^+$  channels, so that the depolarization becomes regenerative, rapidly driving the membrane potential  $V_{\text{m}}$  all the way to the peak of the action potential. The specific value of  $V_{\text{m}}$  at which the net ionic current ( $I_{\text{Na}} + I_{\text{K}} + I_{\text{L}}$ ) changes from outward to inward, depositing a positive charge on the inside of the membrane capacitance, is the threshold.

Early experiments with extracellular stimulation of nerve fibers showed that, for a short time after an action potential (typically a few milliseconds), it is impossible to generate another action potential. This *absolute refractory period* is followed by a period when it is possible to stimulate another action potential, but only with a stimulus larger than what was needed for the first. This *relative refractory period* typically lasts 5 to 10 ms.

The Hodgkin-Huxley analysis provided a mechanistic explanation of two factors underlying the refractory period. In the immediate aftermath of an action potential, it is impossible to evoke another one, even with a very strong stimulus, because the  $\text{Na}^+$  channels remain inactivated. After repolarization,  $\text{Na}^+$  channels recover from inactivation and reenter the resting state, a transition that takes several milliseconds (Figure 10–8). The relative refractory period corresponds to partial recovery from inactivation.

The relative refractory period is also influenced by a residual increase in  $\text{K}^+$  conductance that follows the action potential. It takes several milliseconds for all of the  $\text{K}^+$  channels that open during the action potential to return to their closed state. During this period, when the  $\text{K}^+$  conductance remains somewhat elevated,  $V_{\text{m}}$  is

slightly more negative than its normal resting value, as  $V_{\text{m}}$  approaches  $E_{\text{K}}$  (Figure 10–7, Equation 9–4). This *afterhyperpolarization* and residual increase in  $g_{\text{K}}$  contribute to the increase in depolarizing current required to drive  $V_{\text{m}}$  to threshold during the relative refractory period.

### The Mechanisms of Voltage Gating Have Been Inferred From Electrophysiological Measurements

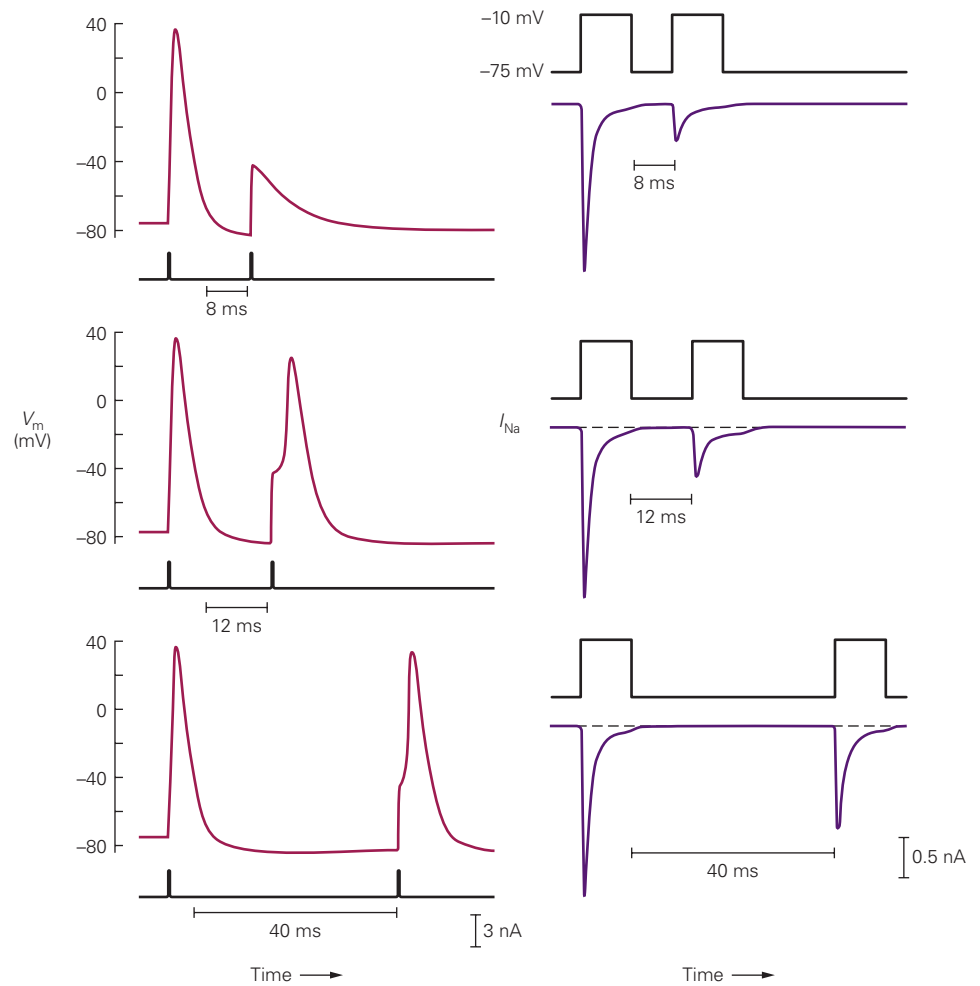
The empirical equations derived by Hodgkin and Huxley are quite successful in describing how the flow of ions through the  $\text{Na}^+$  and  $\text{K}^+$  channels generates the action potential. However, these equations describe the process of excitation in terms of changes in membrane conductance and current. They tell little about the mechanisms that activate or inactivate channels in response to changes in membrane potential or about channel selectivity for specific ions.

We now know that the voltage-dependent conductances described by Hodgkin and Huxley are generated by ion channels that open in a voltage- and time-dependent manner. Patch-clamp recordings from a variety of nerve and muscle cells have provided detailed information about the properties of the voltage-dependent  $\text{Na}^+$  channels that generate the action potential. Recordings of single voltage-gated  $\text{Na}^+$  channels show that, in response to a depolarizing step, each channel opens in an all-or-none fashion, conducting brief current pulses of constant amplitude but variable duration.

Each channel opening is associated with a current of about 1 pA (at voltages near  $-30$  mV), and the open state is rapidly terminated by inactivation. Each channel behaves stochastically, opening after a variable time and staying open for a variable time before inactivating. If the openings of all the channels in a cell membrane in response to a step depolarization are summed or the openings of a single channel to multiple trials of the same depolarization are summed (Figure 10–9), the result is an averaged current with the same time course as the macroscopic  $\text{Na}^+$  current recorded in voltage-clamp experiments (see Figure 10–4B).

To explain how changes in membrane potential lead to an increase in  $\text{Na}^+$  conductance, Hodgkin and Huxley deduced from basic thermodynamic considerations that a conformational change in some membrane component that regulates the conductance must move charged particles through the membrane electric field. As a result, membrane depolarization would exert a force causing the charged particles to move, thereby opening the channel. For a channel with positively charged mobile particles, the depolarization

**Figure 10–8** The refractory period is associated with recovery of the sodium channels from inactivation. *Left:* The voltage response of a mouse dorsal root ganglion neuron to two current pulses (bottom traces). The first triggers an action potential; the second triggers a variable voltage response depending on the delay between the current pulses. *Right:* Sodium currents recorded under voltage clamp in the same cell evoked by two depolarizing voltage pulses separated by the intervals indicated in the records on the left. In this neuron, the refractory period corresponds to the time needed for recovery of about 20% of the sodium channels. (Data from Pin Liu and Bruce Bean.)



would produce an outward movement of charge that should precede the opening of the channel. Upon membrane repolarization the charge would move in the opposite direction, closing the channel. Because the mobile charge movement is confined to the membrane, it is a type of capacitive current. This *gating charge* movement was predicted to generate a small outward current (or *gating current*), which was later confirmed when the membrane current was examined using very sensitive techniques. Blocking the inward ionic current with tetrodotoxin revealed a small outward capacitive current during the time the channels were activating (Figure 10–10A). In later experiments, this gating current ( $I_g$ ) was progressively reduced by mutating the positively charged lysine and arginine residues in the four S4 transmembrane regions of the  $Na^+$  channel to neutral residues. Thus, the gating current is produced by outward movement of the positively charged residues in the S4 regions through the membrane electric field (Chapter 8). Voltage-gated  $K^+$  and  $Ca^{2+}$  channels also generate gating currents during channel opening.

Recent experiments have shown that the four S4 transmembrane regions of the  $Na^+$  channel move with different time courses. Movement of the S4 regions of the first three domains (DI, DII, DIII) occurs first and is associated with channel activation. Movement of the S4 region of domain IV occurs more slowly and is associated with inactivation. Inactivation of  $Na^+$  channels likely involves a series of conformational changes whereby outward movement of the S4 region of domain IV enables binding of the cytoplasmic linker connecting domains III and IV to a binding site near the intracellular ends of the pore-forming S6 helices, stabilizing a nonconducting inactivated state of the pore (Figure 10–10B,C).

Control of channel activation by gating charges results in a characteristic feature of voltage-dependent channels: The conductance change occurs over a relatively narrow range of  $V_m$  with a saturating value for larger depolarizations. When peak  $I_{Na}$  is measured over a wide range of  $V_m$  and then converted to a conductance, as illustrated in Figure 10–6, the voltage dependence of peak conductance has a sigmoid shape (Figure 10–11). Activation of voltage-dependent

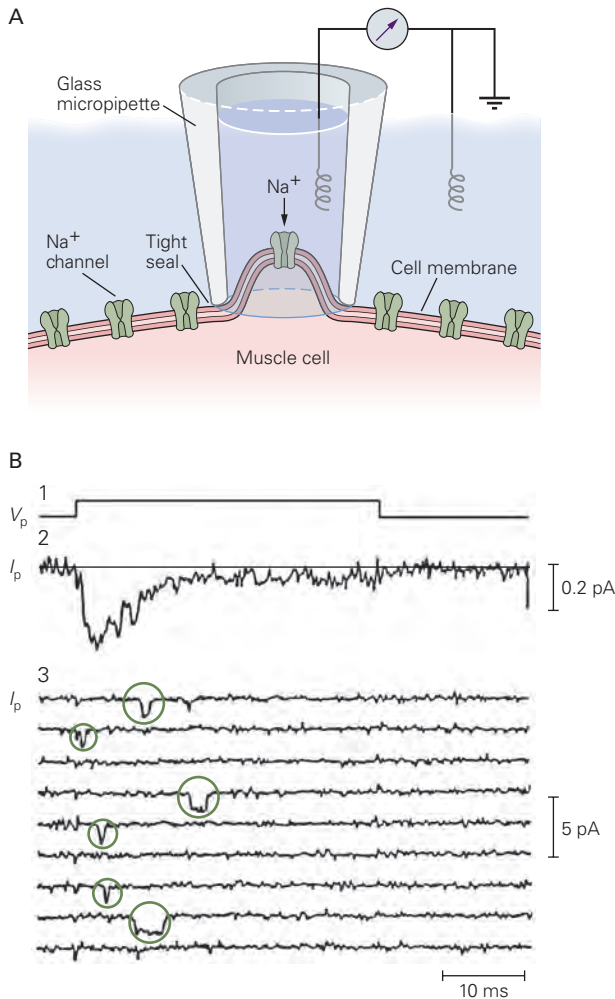


**Figure 10-9** Individual voltage-gated ion channels open in an all-or-none fashion.

**A.** A small patch of membrane containing a single voltage-gated  $\text{Na}^+$  channel is electrically isolated from the rest of the cell by the patch electrode. The  $\text{Na}^+$  current that enters the cell through the channel is recorded by a monitor connected to the patch electrode (see Box 8-1).

**B.** Recordings of single  $\text{Na}^+$  channels in cultured muscle cells of rats. (1) Time course of a 10 mV depolarizing voltage step applied across the isolated patch of membrane ( $V_p$  = potential difference across the patch). (2) The sum of the inward current through the  $\text{Na}^+$  channel in the patch during 300 trials ( $I_p$  = current through the patch). The trace was obtained by blocking the  $\text{K}^+$  channels with tetraethylammonium and subtracting the leakage and capacitive currents electronically. (3) Nine individual trials from the set of 300, showing six openings of the channel (circled). These data demonstrate that the total  $\text{Na}^+$  current recorded in a conventional voltage-clamp record (see Figure 10-3B) can be accounted for by the statistical nature of the all-or-none opening and closing of a large number of  $\text{Na}^+$  channels. (Reproduced, with permission, from Sigworth and Neher 1980.)

sodium conductance begins at about  $-50$  mV (near the threshold for action potential firing), reaches a midpoint near  $-25$  mV, and saturates at about  $0$  mV. The saturation of conductance occurs when the S4 regions of the entire population of  $\text{Na}^+$  channels have moved to the activated conformation.

The relationship of conductance to voltage can be approximately fit by the Boltzmann function, an equation from statistical mechanics that describes the distribution of a population of molecules that can exist in distinct states with different potential energies. In the case of  $\text{Na}^+$  channels, the channels move between closed and open states that differ in potential energy because of the work done when the S4 region gating charges move through the electric field of the membrane (Figure 10-10C). The two parameters of the fitted Boltzmann curve, the midpoint and the slope factor, provide a convenient characterization of the voltage dependence with which channels open. The curve is steeper if more gating charge moves as channels convert between closed and open states. The voltage dependence of activation and inactivation of many other types of voltage-dependent channels can also be approximated by Boltzmann curves with characteristic midpoints and slopes.

### Voltage-Gated Sodium Channels Select for Sodium on the Basis of Size, Charge, and Energy of Hydration of the Ion

In Chapter 8, we saw how the structure of the  $\text{K}^+$  channel pore could explain how such channels are able to select for  $\text{K}^+$  over  $\text{Na}^+$  ions. The narrow diameter of the  $\text{K}^+$  channel selectivity filter (around  $0.3$  nm) requires that a  $\text{K}^+$  or  $\text{Na}^+$  ion must shed nearly all of its waters of hydration to enter the channel, an energetically unfavorable event.

The energetic cost of dehydration of a  $\text{K}^+$  ion is well compensated by its close interaction with a cage of electronegative carbonyl oxygen atoms contributed by the peptide backbones of the four subunits of the  $\text{K}^+$  channel selectivity filter. Because of its smaller radius, a  $\text{Na}^+$  ion has a higher local electric field than does a  $\text{K}^+$  ion and therefore interacts more strongly with its waters of hydration than does  $\text{K}^+$ . On the other hand, the small diameter of the  $\text{Na}^+$  ion precludes close interaction with the cage of carbonyl oxygen atoms in the selectivity filter; the resultant high energetic cost of dehydrating the  $\text{Na}^+$  ion excludes it from entering the channel.

How then does the selectivity filter of the  $\text{Na}^+$  channel select for  $\text{Na}^+$  over  $\text{K}^+$  ions? Bertil Hille deduced a model for the  $\text{Na}^+$  channel's selectivity mechanism from measurements of the channel's relative

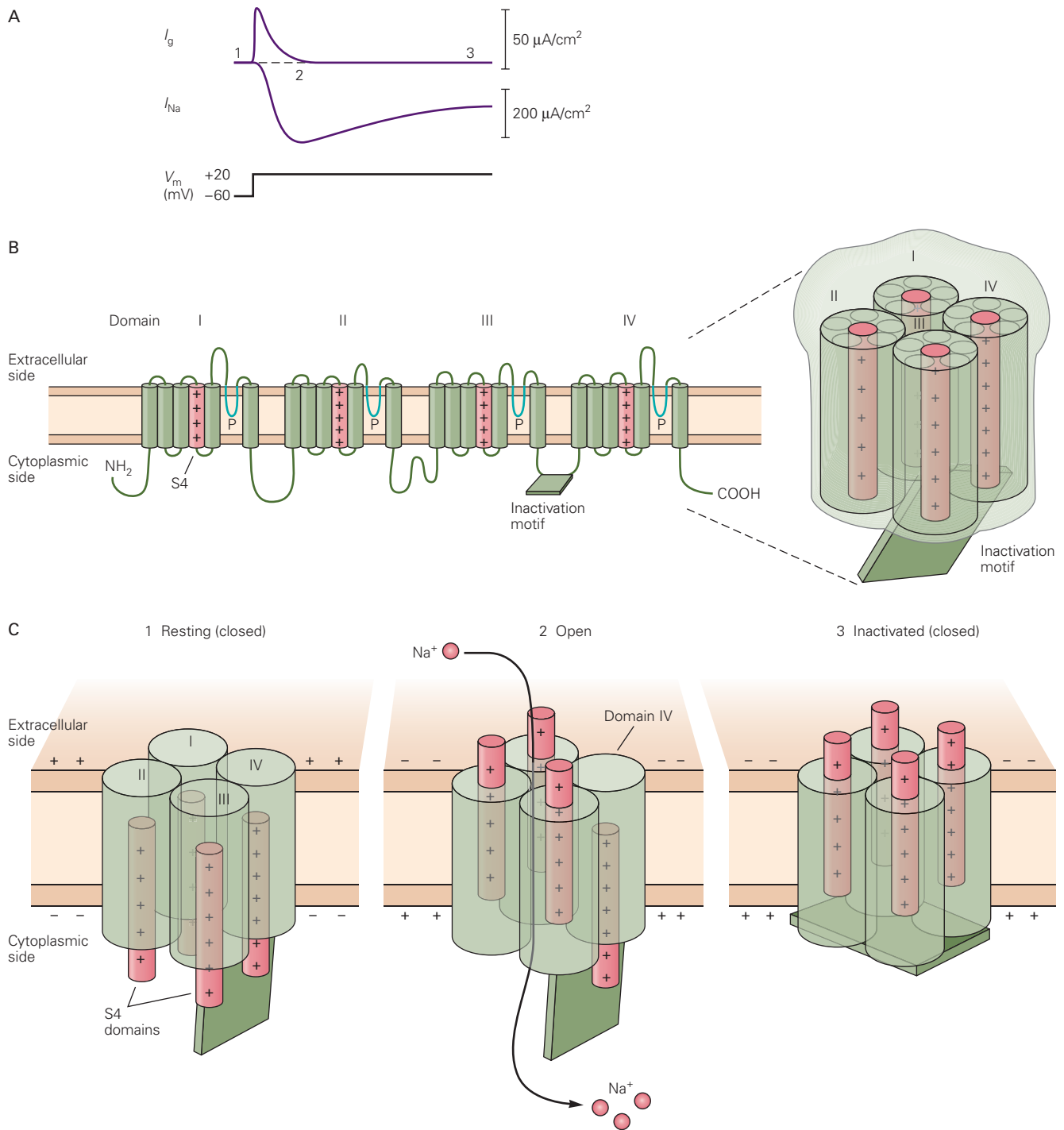


**Figure 10-10** The opening and closing of the sodium channel are associated with a redistribution of charges.

**A.** When the membrane is depolarized, the  $\text{Na}^+$  current ( $I_{Na}$ ) is activated and then inactivated. The activation of the  $\text{Na}^+$  current is preceded by a brief capacitive *gating current* ( $I_g$ ), reflecting the outward movement of positive charges within the walls of the  $\text{Na}^+$  channels. To detect this small gating current, it is necessary to block the flow of ionic current through the  $\text{Na}^+$  and  $\text{K}^+$  channels and subtract the capacitive current that depolarizes the lipid bilayer. (Adapted, with permission, from Armstrong and Gilly 1979.)

**B.** Secondary structure of the  $\alpha$ -subunit of mammalian sodium channels showing location of gating charges. The sodium channel  $\alpha$ -subunit is a single polypeptide consisting of four repeated domains, each containing six transmembrane regions. The fourth transmembrane region (S4 region) of each domain contains positively charged arginine and lysine residues that form

the gating charge of the channels. (Adapted, with permission, from Ahern et al. 2016. Permission conveyed through Copyright Clearance Center, Inc.)

**C.** Diagrams depict the redistribution of gating charge and positions of the activation and inactivation gates when the channel is at rest, open, and inactivated. The red cylinders represent the S4 regions containing the positive gating charges. Depolarization of the cell membrane from the resting state causes the gating charge to move outward. Outward movement of the S4 regions of domains I, II, and III is associated with activation (1–2), whereas slower movement of the S4 region of domain IV is associated with inactivation (2–3). The movement of the S4 region of domain IV allows an intracellular loop between domains III and IV (depicted as a green rectangle) to bind to a docking site near the S6 helices at the inside of the pore, allosterically stabilizing an inactivated closed state. (Adapted from Ahern et al. 2016.)

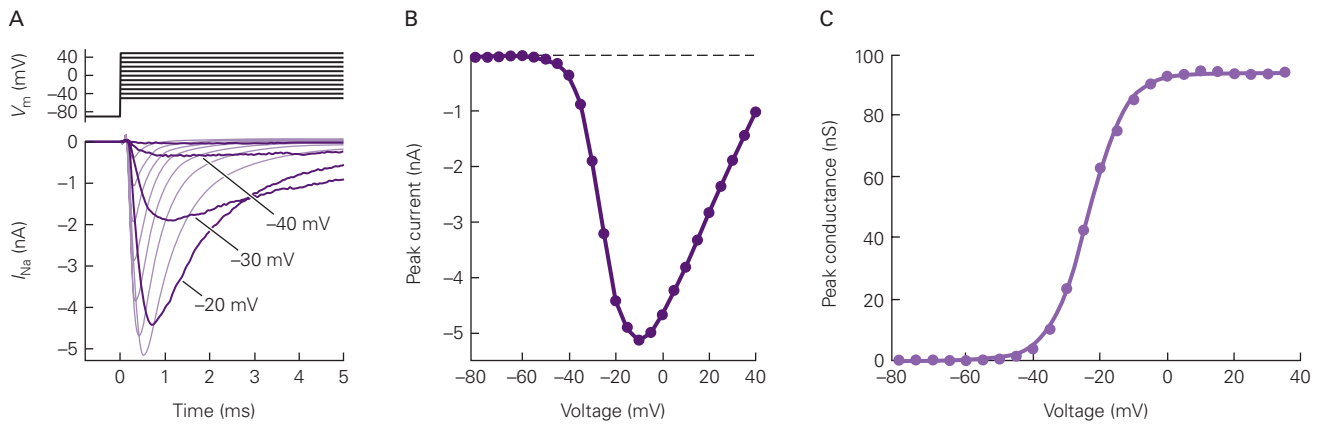


**Figure 10-11** The voltage dependence of sodium channel activation is determined by the number of gating charges.

**A.** Whole-cell patch-clamp recordings of voltage-gated Na<sup>+</sup> currents were made in a dissociated hippocampal pyramidal neuron. Sodium channel currents were isolated by blocking currents through K<sup>+</sup> and Ca<sup>2+</sup> channels and then subtracting the capacitive and leakage currents that remained after blocking Na<sup>+</sup> currents.

**B.** Current-voltage curve for peak Na<sup>+</sup> current.

**C.** Peak Na<sup>+</sup> conductance versus membrane potential.

Increases in peak  $g_{Na}$  in response to a series of depolarizing voltage steps were calculated from peak current, as in Box 10-2. The experimental data points are fit by the Boltzmann relation with the form  $g_{Na}/g_{Na(max)} = 1/[1 + \exp(-(V_m - V_n)/k)]$ , where  $V_n = -24$  mV is the midpoint of the activation curve and  $k = 5.5$  is the “slope factor,” with units of mV, and  $g_{Na(max)}$  is the maximal sodium conductance at positive voltages. The greater the number of gating charges that must move to open the channel, the smaller is the slope factor. The voltage dependence of most voltage-gated channels can be fit by similar Boltzmann curves. (Data from Indira M. Raman.)

permeability to a range of organic and inorganic cations. As we learned in Chapter 8, the channel behaves as if it contains a selectivity filter, or recognition site, which selects partly on the basis of size, thus acting as a molecular sieve (see Figure 8-1). Based on the size and hydrogen-bonding characteristics of the largest organic cation that could readily permeate the channel, Hille deduced that the selectivity filter has rectangular dimensions of  $0.3 \times 0.5$  nm. This cross section is just large enough to accommodate one Na<sup>+</sup> ion contacting one water molecule (see Figure 8-1). Because a K<sup>+</sup> ion in contact with one water molecule is larger than the size of the selectivity filter, it cannot readily permeate.

According to Hille’s model, negatively charged carboxylic acid groups of glutamate or aspartate residues at the outer mouth of the pore perform the first step in the selection process by attracting cations and repelling anions. The negative carboxylic acid groups, as well as other oxygen atoms that line the pore, can substitute for waters of hydration, but the degree of effectiveness of this substitution varies among ion species. The negative charge of a carboxylic acid is able to form a stronger coulombic interaction with the smaller Na<sup>+</sup> ion than with the larger K<sup>+</sup> ion. Because the Na<sup>+</sup> channel is large enough to accommodate a cation in contact with several water molecules, the energetic cost of dehydration is not as great as it is in a K<sup>+</sup> channel. As a result of these two features, the Na<sup>+</sup> channel is able

to select for Na<sup>+</sup> over K<sup>+</sup>, but not perfectly, with  $P_{Na}/P_K \sim 12/1$ . Structures of bacterial and vertebrate voltage-gated Na<sup>+</sup> channels obtained by X-ray crystallography and cryo-electron microscopy have confirmed many of the key features of Hille’s model.

### Individual Neurons Have a Rich Variety of Voltage-Gated Channels That Expand Their Signaling Capabilities

The basic mechanism of electrical excitability identified by Hodgkin and Huxley in the squid giant axon is common to most excitable cells: Voltage-gated channels conduct an inward Na<sup>+</sup> current followed by an outward K<sup>+</sup> current. However, we now know that the squid axon is unusually simple in expressing only two types of voltage-gated ion channels. In contrast, the genomes of both vertebrates and invertebrates include large families of voltage-gated Na<sup>+</sup>, K<sup>+</sup>, and Ca<sup>2+</sup> channels encoded by sub-families of related genes that are widely expressed in different kinds of nerve and muscle cells.

A neuron in the mammalian brain typically expresses a dozen or more different types of voltage-gated ion channels. The voltage dependence and kinetic properties of various Na<sup>+</sup>, Ca<sup>2+</sup>, and K<sup>+</sup> channels can differ widely. Moreover, the distribution of these



channels varies between different types of neurons and even between different regions of a single neuron. The great variety of voltage-gated channels in the membranes of most neurons enables a neuron to fire action potentials with a much greater range of frequencies and patterns than is possible in the squid axon, and thus allows much more complex information-processing abilities and modulatory control than is possible with just two types of channels.

### The Diversity of Voltage-Gated Channel Types Is Generated by Several Genetic Mechanisms

The conservative mechanism by which evolution proceeds—creating new structural or functional entities by duplicating, modifying, shuffling, and recombining existing gene-coding sequences—is illustrated by the diversity and modular design of the members of the extended gene superfamily that encodes the voltage-gated  $\text{Na}^+$ ,  $\text{K}^+$ , and  $\text{Ca}^{2+}$  channels. This family also includes genes that encode calcium-activated  $\text{K}^+$  channels, the hyperpolarization-activated HCN non-selective cation channels, and a voltage-independent cyclic nucleotide-gated cation channel important for phototransduction and olfaction.

The functional differences between these channels are produced by differences in amino acid sequences in their core transmembrane domains as well as by the addition of regulatory elements in cytoplasmic domains. For example, some  $\text{K}^+$  channels have a mechanism of inactivation mediated by a tethered plug formed by the cytoplasmic N-terminus of the channel protein, which binds to the inner mouth of the channel when the activation gate opens. The C-terminal cytoplasmic end of the channel proteins is a particularly rich locus for regulatory elements, including domains that bind either  $\text{Ca}^{2+}$  or cyclic nucleotides, enabling these agents to regulate channel gating. Inward-rectifying  $\text{K}^+$  channels, which are tetramers of subunits with only a P-region and flanking transmembrane regions, have an internal cation-binding site that produces rectification. When the cell is depolarized, cytoplasmic  $\text{Mg}^{2+}$  or positively charged polyamines (small organic molecules that are normal constituents of the cytoplasm) are electrostatically driven to this binding site from the cytoplasm, plugging the channel (Figure 10–12).

Figure 10–12 represents large families of channels within which there is considerable structural and functional diversity. Five different mechanisms contribute to diversity in voltage-gated channels.

1. Multiple genes encode related principal subunits within each class of channel. For example,

in mammalian neurons and muscle, at nine different genes encode voltage-gated  $\text{Na}^+$  channel  $\alpha$ -subunits.

2. The four  $\alpha$ -subunits that form a voltage-gated  $\text{K}^+$  channel (Figure 8–11) can be encoded by different genes. After translation, the  $\alpha$ -subunits are in some cases mixed and matched in various combinations, thus forming different subclasses of heteromeric channels.
3. A single gene product may be alternatively spliced, resulting in variations in the messenger RNA (mRNA) molecules that encode the  $\alpha$ -subunit.
4. The mRNA that encodes an  $\alpha$ -subunit may be edited by chemical modification of a single nucleotide, thereby changing the composition of a single amino acid in the channel subunit.
5. Principal pore-forming  $\alpha$ -subunits of all channel types are commonly combined with different accessory subunits to form functionally different channel types.

These accessory subunits (often termed  $\beta$ -,  $\gamma$ -, or  $\delta$ -subunits) may be either cytoplasmic or membrane-spanning and can produce a wide range of effects on channel function. For example, some  $\beta$ -subunits enhance the efficiency with which the channel protein is transported from the rough endoplasmic reticulum to the membrane, as well determining its final destination on the cell surface. Other subunits can regulate the voltage sensitivity or kinetics of channel gating. In contrast to the  $\alpha$ -subunits, there is no known homology among the  $\beta$ -,  $\gamma$ -, and  $\delta$ -subunits from the three major subfamilies of voltage-gated channels.

These various sources of channel diversity also vary widely between different areas of the nervous system, between different types of neurons, and within different subcellular compartments of a given neuron. A corollary of this regional differentiation is that mutations or epigenetic mechanisms that alter voltage-gated channel function can have very selective effects on neuronal or muscular function. The result is a large array of neurological diseases called channelopathies (Chapters 57 and 58).

### Voltage-Gated Sodium Channels

The  $\alpha$ -subunits of mammalian voltage-dependent  $\text{Na}^+$  channels are encoded by nine genes. Three of the  $\alpha$ -subunits encoded by these genes (Nav1.1, Nav1.2, and Nav1.6) are widely expressed in neurons in the mature mammalian brain, while four others have more restricted expression in neurons. Nav1.3 is strongly expressed early in development, with little expression in the mature brain, but can be reexpressed in injured

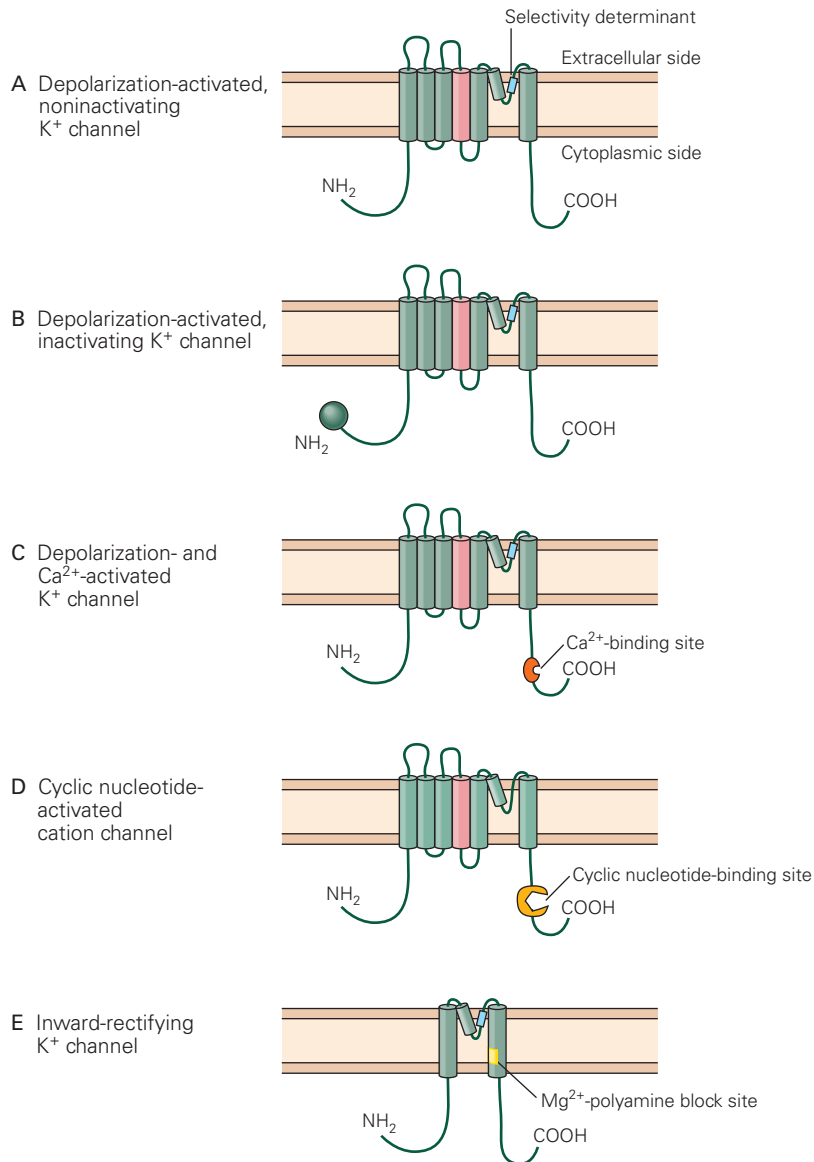


**Figure 10-12** The extended gene family of voltage-gated channels produces variants of a common molecular design.

**A.** The basic transmembrane topology of an  $\alpha$ -subunit of a voltage-gated  $K^+$  channel. The S4 membrane-spanning  $\alpha$ -helix is labeled in red.

**B.** Many  $K^+$  channels that are first activated and then inactivated by prolonged depolarization have a ball-and-chain segment at their N-terminal end that inactivates the channel by plugging its inner mouth.

**C.** Some  $K^+$  channels that require both depolarization and an increase in intracellular  $Ca^{2+}$  to activate have a  $Ca^{2+}$ -binding sequence attached to the C-terminal end of the channel.

**D.** Cation channels gated by cyclic nucleotides have a cyclic nucleotide-binding domain attached to the C-terminal end. One

subclass of such channels includes the voltage-independent, cyclic nucleotide-gated channels important in the transduction of olfactory and visual sensory signals. Another subclass consists of the hyperpolarization-activated cyclic nucleotide-gated (HCN) channels important for pacemaker activity (see Figure 10-15D). The P loops in these channels lack key amino acid residues required for  $K^+$  selectivity. As a result, these channels do not show a high degree of discrimination between  $Na^+$  and  $K^+$ .

**E.** Inward-rectifying  $K^+$  channels, which are gated by blocking particles available in the cytoplasm, are formed from a truncated version of the basic building block, with only two membrane-spanning regions and a P-region.

tissue, for example following spinal cord injury. Nav1.7 channels are confined to autonomic and sensory neurons in the peripheral nervous system. Nav1.8 and Nav1.9 channels are largely restricted to a subset of peripheral sensory neurons, with particularly prominent expression in pain-sensing primary sensory neurons (nociceptors). Nav1.1, Nav1.2, Nav1.3, Nav1.6, and Nav1.7 channels have generally similar voltage dependence and relatively fast activation and inactivation kinetics compared to Nav1.8 and Nav1.9 channels. Nav1.4 channels in skeletal muscle fibers and Nav1.5 channels in cardiac muscle conduct the voltage-gated  $\text{Na}^+$  current that generates action potentials in these tissues.

Although Nav1.1, Nav1.2, and Nav1.6 are all widely expressed in mammalian central neurons, they are expressed in different proportions in different types of neurons. Nav1.1 channels are particularly strongly expressed in some inhibitory GABAergic interneurons, and some loss-of-function mutations in Nav1.1 channels can lead to epilepsy, as in Dravet syndrome, perhaps reflecting greater loss of excitability of inhibitory neurons relative to excitatory neurons.

### Voltage-Gated Calcium Channels

Virtually all neurons contain voltage-gated  $\text{Ca}^{2+}$  channels that open in response to membrane depolarization. A strong electrochemical gradient drives  $\text{Ca}^{2+}$  into the cell, so these channels give rise to an inward current that helps depolarize the cell.

A single neuron typically expresses at least four or five different types of voltage-gated  $\text{Ca}^{2+}$  channels with different voltage dependence, kinetic properties, and subcellular localization. Calcium channels that are widely expressed in central and peripheral neurons include Cav1.2 and Cav1.3 channels (collectively known as L-type channels), Cav2.1 (P/Q-type channels), Cav2.2 (N-type channels), and Cav2.3 (R-type channels). The various Cav1 and Cav2 family channels are collectively known as *high-threshold* or *high-voltage activated* (HVA)  $\text{Ca}^{2+}$  channels because activation generally requires relatively large depolarizations.

Members of the Cav3 family, collectively known as *T-type* or *low-voltage activated* (LVA) channels, are more selectively expressed in certain neurons. They are opened by small depolarizations (as negative as  $-65$  mV) and undergo inactivation over tens of milliseconds. At normal resting potentials, Cav3 channels are typically inactivated. Hyperpolarization of the membrane voltage (as by inhibitory synaptic input) removes resting inactivation, which enables transient activation of the LVA channels following the hyperpolarization as the membrane voltage moves back toward its resting

level. This activation can produce a regenerative depolarization that triggers a burst of  $\text{Na}^+$  action potentials, which terminates when the Cav3 channels inactivate. Such postinhibitory burst firing is common in some regions of the thalamus and can help drive synchronized burst firing in neural circuits (see Figure 44–2). Similar rebound activation of Cav3 channels following the hyperpolarizing phase of a slow pacemaker potential contributes to spontaneous rhythmic bursting in some thalamocortical neurons (see Figure 10–15).

### Voltage-Gated Potassium Channels

Voltage-dependent  $\text{K}^+$  channels comprise an especially varied group of channels that differ in their kinetics of activation, voltage-activation range, and sensitivity to various ligands. Mammalian neurons typically express members of at least five families of voltage-dependent  $\text{K}^+$  channels: Kv1, Kv2, Kv3, Kv4, and Kv7 (Figure 10–13). Each family consists of multiple gene products, with each channel composed of four  $\alpha$ -subunits. For example, there are eight closely-related genes encoding the members of the Kv1 gene family (Kv1.1–Kv1.8).

The subunits can be of the same type (a homomeric channel) or of different gene products from within the same Kv family (a heteromeric channel). For example, Kv1 channels can be formed by heteromeric combinations of at least five different gene products that have wide expression in central neurons, with each combination possessing different properties of kinetics and voltage dependence. The possible functional variation provided by different combinations of  $\alpha$ -subunits in heteromeric channels is immense, although not all possible combinations actually occur.

One way of distinguishing different components of voltage-dependent  $\text{K}^+$  currents in a neuron is by the presence or absence of inactivation. Non-inactivating  $\text{K}^+$  current, like that described in the squid axon by Hodgkin and Huxley, is called *delayed rectifier*  $\text{K}^+$  current. In the squid axon, delayed rectifier current flows through a single Kv1 family channel type. In most mammalian neurons, delayed rectifier current includes multiple components from Kv1, Kv2, and Kv3 family channels, each with different kinetics and voltage dependence. Kv3 channels are unusual in requiring large depolarizations to become activated and also in having very rapid kinetics of activation. As a result, Kv3 channels are not activated until the action potential is near its peak, but they activate quickly enough to help terminate the action potential.

In addition to delayed rectifier current, many neurons also have a component of inactivating  $\text{K}^+$  current known as A-type current. In cell bodies and dendrites,



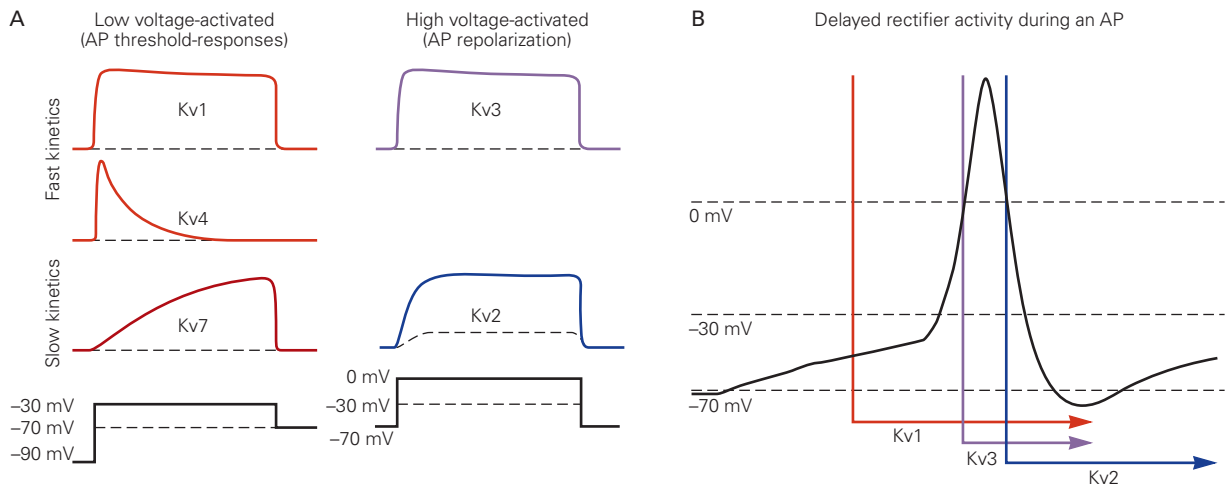


**Figure 10-13** Different voltage dependence and kinetics of major classes of mammalian voltage-activated potassium channels.

**A.** Simplified generalization of the voltage dependence and kinetics of the major voltage-gated  $K^+$  families. Because Kv1, Kv4, and Kv7 channels can be activated by relatively small depolarizations, they often help control action potential (AP) threshold. Kv2 and Kv3 channels require larger depolarizations to be activated. Kv1, Kv3, and Kv4 channels are activated relatively rapidly, whereas Kv7 and Kv2 channels are activated more slowly.

A-type current is formed primarily by Kv4 family  $\alpha$ -subunits, which form channels that inactivate over a range of time scales from a few milliseconds to tens of milliseconds. Kv1 channels that include Kv1.4 subunits or the auxiliary subunit Kv $\beta$ 1 also mediate an inactivating component of current, which is highly expressed in some nerve terminals as well as some cell bodies.

As is the case for  $Na^+$  channels and Cav3 family channels, A-type  $K^+$  current not only inactivates during large depolarizations but is also subject to steady-state inactivation by small depolarizations from rest, providing a mechanism by which its amplitude can be modulated by small voltage changes around resting potential (see Figure 10-15B).

Kv7 subunits form non-inactivating channels that require only small depolarizations from rest to be activated and can even be activated significantly at the resting potential. In some neurons, Kv7 channels are downregulated by the transmitter acetylcholine acting through muscarinic G protein-coupled receptors (thus the origin of an alternative name of “M-current”). Kv7 channels typically activate relatively slowly, over tens of milliseconds, and provide little current during a single action potential but tend to suppress firing of subsequent action potentials (Chapter 14).

The KCNH gene family consists of three subfamilies of voltage-gated  $K^+$  channels (Kv10, Kv11, and

**B.** Simplified generalization of the differing activation times of the major components of delayed rectifier  $K^+$  channels during an action potential. Kv1 channels require small depolarizations and are activated rapidly, sometimes significantly in advance of the action potential. Kv3 channels require large depolarizations and are activated late in the rising phase of the action potential and deactivated very rapidly thereafter. Kv2 channels are activated relatively slowly during the falling phase of the action potential and remain open during the afterhyperpolarization. (Adapted, with permission, from Johnston et al. 2010.)

Kv12), which are also expressed in the brain. They influence resting potential, action potential threshold, and frequency and pattern of firing.

### Voltage-Gated Hyperpolarization-Activated Cyclic Nucleotide-Gated Channels

Many neurons have cation channels that are slowly activated by hyperpolarization. This sensitivity to hyperpolarization is enhanced when intracellular cyclic nucleotides bind to the channel. Because these hyperpolarization-activated cyclic nucleotide-gated (HCN) channels have only two of the four negative binding sites found in the selectivity filter of  $K^+$  channels, they are permeable to both  $K^+$  and  $Na^+$  and have a reversal potential around  $-40$  to  $-30$  mV. As a result, hyperpolarization from rest, as during strong synaptic inhibition or following an action potential, opens the channels to generate an inward depolarizing current referred to as  $I_h$  (see Figure 10-15D).

### Gating of Ion Channels Can Be Controlled by Cytoplasmic Calcium

In a typical neuron, the opening and closing of certain ion channels can be modulated by various cytoplasmic factors, thus affording the neuron's excitability